

Statistical Physics in Modeling Chromosome Movements During Nuclear Oscillation of Fission Yeast



Wenwen Huang

Max Planck Institute for the Physics of Complex Systems
TU Dresden

This dissertation is submitted for the degree of
Doctor of Philosophy

January 2017

I would like to dedicate this thesis to my loving parents ...

Declaration

I hereby declare that except where specific reference is made to the work of others, the contents of this dissertation are original and have not been submitted in whole or in part for consideration for any other degree or qualification in this, or any other university. This dissertation is my own work and contains nothing which is the outcome of work done in collaboration with others, except as specified in the text and Acknowledgements. This dissertation contains fewer than 65,000 words including appendices, bibliography, footnotes, tables and equations and has fewer than 150 figures.

Wenwen Huang
January 2017

Acknowledgements

And I would like to acknowledge ...

Abstract

This is where you write your abstract ...

Table of contents

List of figures	xv
List of tables	xvii
1 Introduction	1
1.1 Nuclear oscillation in fission yeast	1
1.1.1 Fission yeast	2
1.1.2 Basis of meiosis	3
1.1.3 Nuclear oscillation	5
1.1.4 The role of nuclear oscillation	6
1.2 Chromosomes modeled as the polymer	6
1.2.1 The ring polymer model	7
1.2.2 Pulled polymer model	10
1.3 Outline	11
1.3.1 Research goals	11
1.3.2 Overview of the thesis	12
2 The Model and Simulation Methods	13
2.1 The pulled polymer loop model	13
2.1.1 Coordinate transformation	14
2.1.2 The bead-rod model	14
2.1.3 The bead-spring model	18
2.2 The Brownian Dynamics simulation method	20
2.2.1 BD simulation of the bead-rod model	20
2.2.2 BD simulation of the bead-spring model	21
2.3 The Monte-Carlo simulation of the bead-rod model	21
2.4 Summary	21

3 Simulation Methods	23
3.1 Brownian Dynamics Simulation of the Bead-rod Model	23
3.1.1 Predictor-corrector Algorithm	23
3.1.2 The Pseudo Force	23
3.2 Monte-Carlo Simulation of the Bead-rod Model	23
3.3 Brownian Dynamics Simulation of the Bead-spring Model	23
3.3.1 Euler Algorithm and Stochastic Runge-Kutta Algorithm	23
3.3.2 Excluded volume	23
3.3.3 Bending Potential	23
3.4 Monte-Carlo Simulation of the Particle Hopping Model	23
3.4.1 Classical Monte-Carlo	23
3.4.2 Kinetic Monte-Carlo	23
3.5 Summary	23
4 Equilibrium Statistics	25
4.1 Pinned Polymer Loop Model	26
4.1.1 Polymer Loop Moving in One Direction	26
4.1.2 Pinned Polymer Loop in Constant Force Field	26
4.2 Pinned Polymer Loop in 1D	26
4.2.1 Mapping to Particles on 1D Lattice	26
4.2.2 The Grand Canonical Ensemble Solution	26
4.2.3 Canonical Ensemble Solution	26
4.3 Equilibrium Statistics in 3D	26
4.3.1 The Mean of Bead Position	26
4.3.2 The Variance of Bead Position	26
4.4 Two intersecting Loops	26
4.5 Back to the Biological Problem	26
4.6 Summary	26
5 Dynamical Properties	27
5.1 Rouse Theory of the Pinned Bead-spring Loop	27
5.1.1 The Normal Modes	27
5.1.2 Relaxation Time	27
5.2 1D Pinned Bead-rod Loop Maps to ASEP	27
5.3 The Bethe-ansatz Solution of ASEP	27
5.3.1 Solution of Single Particle	27
5.3.2 Solution of Two Particles	27

5.3.3	Solution of General N particles	27
5.3.4	Relaxation Time	27
5.4	Relaxation Time of 3D Pinned Bead-rod Loop	27
5.5	The Single-file Diffusion	27
5.6	Summary	27
6	Characterize the Nuclear Oscillation	29
6.1	Oscillation of the Pinned Polymer Loop	29
6.1.1	The Rouse Theory	29
6.1.2	Simulation Results	29
6.2	Characterize the Shape of Chromosomes	29
6.2.1	The Gyration Tensor	29
6.2.2	Asphericity and the Nature of Asphericity	29
6.3	Extract Shape Information From Experimental Data	29
6.3.1	Shape from Experimental Data	29
6.3.2	Compare to Theory and Simulation Results	29
6.4	Summary	29
7	Conclusions and Outlook	31
7.1	Conclusions	31
7.2	Outlook	31
Appendix A	The Toeplitz Matrix	33
Appendix B	The Bethe-ansatz Solution of Periodic ASEP	35
References		37

List of figures

1.1	Microscopic view of a fission yeast culture. The scalar bar indicates 10 μm . Image reprinted from [1] with permission.	2
1.2	Overview of meiosis and an illustration of recombination between homologous chromosomes resulting in four unique daughter cells. Image reprinted from [] with permission.	3
1.3	The meiotic prophase I of fission yeast. Telomeres are clustered to form a bouquet structure. Image modified and reprinted from [2].	4
1.4	Time-lapse experiments of nuclear oscillation in fission yeast, DNA marker in green (Rec8-GFP) and SPB marker in magenta (Sid4-mCherry) also indicated by asterisk. Reprinted from [3] with permission.	5
1.5	The sketch of our pulled polymer loops model for chromosomes in meiotic fission yeast. Three pairs of chromosomes with all ends bound to SPB (shown in magenta) in the nucleus are indicated by different colors. The SPB is pulled by multiple dynein motors (not shown) walking along microtubules (dark green). The SPB is anchored to the nuclear envelope (light green) and entrains the whole nucleus.	7
1.6	Illustration of “stem-flower” picture for pulled polymer chain. (a) Trumpet picture at moderate pulling force; (b) Stem-flower picture at strong pulling force. Image reprinted from [4].	10
2.1	Illustration of coordinate transformation. (a) a pulled polymer loop before transformation; (b) pinned polymer loop in an external field after transformation.	14
2.2	Sketch of the bead-rod loop model. The magenta bead represents the SPB and other cyan beads represent the chromosome segments.	15
2.3	The distribution of included angle of a bead-rod trimer. (a) without <i>pseudo</i> force; (b) with <i>pseudo</i> force. The blue bins are from Brownian Dynamics simulation results. Inset of (a) is a sketch for the trimer.	17

List of tables

1.1 Parameters of fission yeast during meiosis	6
--	---

Chapter 1

Introduction

Many biological processes can be transferred to well-studied models in statistical physics. Examples are ranging from the random walk model of mRNA during the transcription [5–7] to the evolution of ecological systems [8–11]. Analysis of these extracted models could help us to get useful insights into the corresponding biological problems. In this thesis, we are interested in modeling a molecular level biological problem, i.e. the motion of chromosomes in fission yeast during meiotic cell division [12–14].

Interestingly, during Prophase I of meiotic fission yeast, the nucleus containing three pairs of chromosomes move from one pole of the rod-like cell to the other, forming an oscillation behavior last for about two hours. The period of the oscillation is about 10 minutes. Cells are divided into two after the oscillation is done [15–17].

We are going to model this oscillation processes quantitatively with the chromosomes represented by polymer models [18, 19]. The results we obtained from the modeling are used to explain relevant biological functionalities like chromosome alignment and gene recombinations [20].

In this chapter, we will introduce the biological backgrounds and some previous related studies about modeling chromosomes with polymers. We will propose our research goals and give an overview of the thesis in the last section.

1.1 Nuclear oscillation in fission yeast

In this section, we will introduce the biological basis of nuclear oscillation in fission yeast. We will firstly introduce our model organism, fission yeast. And then we show some basis of meiosis cell division. Next, we go into the nuclear structure of fission yeast and the movements of chromosomes, specifically during meiosis. The biological processes like

chromosome alignment and recombination are discussed. In the last subsection, we discuss some understandings for the biological role of the nuclear oscillation.

1.1.1 Fission yeast

Fission yeast, also named *Schizosaccharomyces pombe*, is a model organism that widely used in the study of molecular and cell biology. It is a unicellular eukaryote and has a rod-like shape. Typical size of fission yeast is 3-4 micrometres in diameter and 7-14 micrometres in length [21, 22]. See in Fig. 1.1 for a illustration of fission yeast.

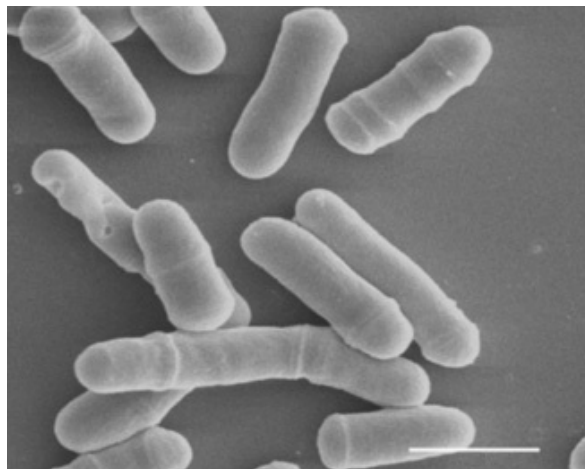


Fig. 1.1 Microscopic view of a fission yeast culture. The scalar bar indicates $10 \mu\text{m}$. Image reprinted from [1] with permission.

Fission Yeast is widely used in traditional brewing and baking. It was first discovered in 1893 in the sediment of millet beer [22, 23]. As a single-celled fungus, fission yeast has a simple genome with three different chromosomes. The genome of fission yeast is fully sequenced and the three chromosomes contain about 14Mb of DNA [24]. It has a rapid growth rate and easily manipulated to make mutants, which make it a perfect modeling organism for genetic studies. The growth of the fission yeast is simply by the elongation at the ends. After mitosis, division occurs by the formation a cell plate that cleaves the cell at its midpoint [21].

Fission yeast is normally a haploid cell. However, when put under stressful conditions, such as nitrogen deficiency, two cells will conjugate to form a diploid and then form four spores via meiosis [25]. This is easy to observe experimentally and this stage is exactly when the interesting nuclear oscillation happens [12]. In the next subsection, we will explain the basis of the meiosis in fission yeast.

1.1.2 Basis of meiosis

Meiosis is a kind of cell division that reduces the number of chromosomes in the parent cell by half and produces four genetically distinct gamete cells. This process occurs in all the sexually reproducing organisms, including human [26].

Meiosis begins with a parent cell with two copies of each chromosome, and is followed by two rounds of cell divisions which produce four potential daughter cells, each has half number of chromosomes as their parent cell. The two rounds of cell division are called *Meiosis I* and *Meiosis II*, respectively. It is during Meiosis I that the pair of chromosomes, one from the father and the other from the mother, separates into two offspring cells. Meiosis II is very similar to the mitosis where two sister chromatins separate [26, 27]. See an overview of meiosis in Fig. 1.2.

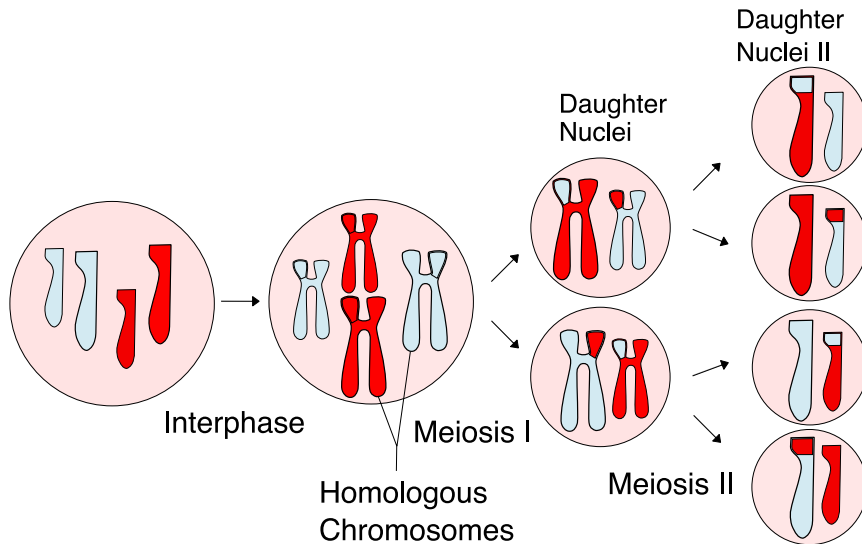


Fig. 1.2 Overview of meiosis and an illustration of recombination between homologous chromosomes resulting in four unique daughter cells. Image reprinted from [] with permission.

As in mitosis, each round of cell division can be divided in prophase, metaphase, anaphase, and telophase. We will elaborate Meiosis I in details, especially the Prophase I when the nuclear oscillation happens.

Prophase I: prophase I is an important stage that many processes happened. Two of the examples are bouquet formation [28] and homologous recombination [29, 17], both occurring in generic organisms. In the early state of Prophase, chromosomes are reorganized spatially, usually, the telomeres are clustered and attached to a small region of the nuclear membrane, forming a bouquet structure. This is called bouquet formation or telomere clustering in biology [12, 28, 30], see in Fig 1.3 for an example in fission yeast. In the process of recombination, the homologous chromosomes, which are paternal and maternal

pairs, align and exchange some parts of their DNA and usually results in the chromosomal crossover. Homologous recombination is critical for pairing and accurate segregation of the chromosomes in the later stage of Meiosis I. More interestingly, this stage is exact the period when the nuclear oscillation happens in fission yeast [31, 32]. We will devote this part to next subsection.

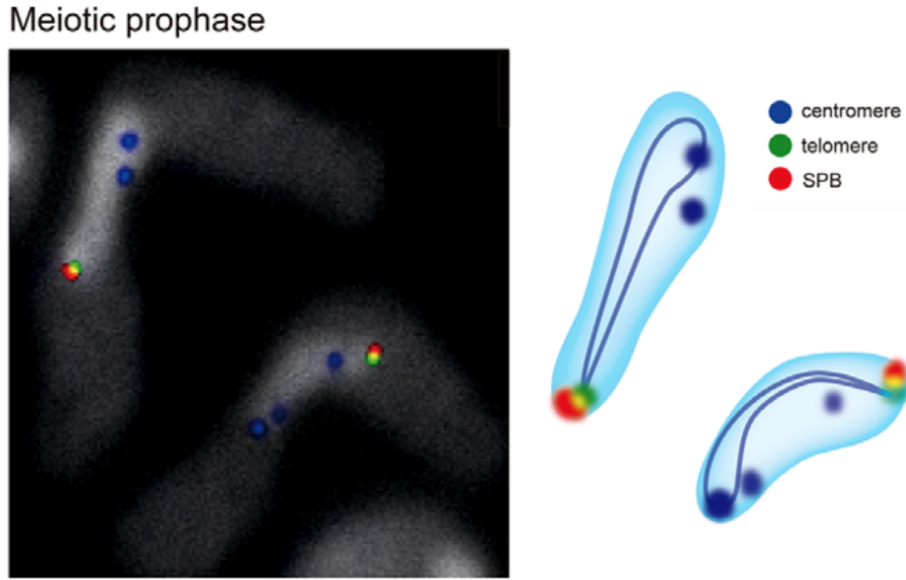


Fig. 1.3 The meiotic prophase I of fission yeast. Telomeres are clustered to form a bouquet structure. Image modified and reprinted from [2].

Metaphase I: in this stage, homologous pairs move together along the middle plate, the microtubules from centrosomes attach to their respective chromosomes, the paired homologous chromosomes align along an equatorial plane that bisects the spindle. However, in Fission Yeast, the centromere is replaced by a functional equivalent organelle called spindle pole body (SPB) [26].

Anaphase I: in this stage, the microtubules shorten, pulling homologous chromosomes to opposite poles. Notice here, chromosomes still consist of a pair of sister chromatids. The cell body elongates, preparing for cell division [26].

Telophase I: in the last stage of Meiosis I, chromosomes arrive at the poles. The microtubules network of spindle disappears. New nuclear membrane appears. The two daughter cells now only have half the number of chromosomes [26].

After Meiosis I, Meiosis II occurs without DNA replication in between. The process is similar to Meiosis I except the sister chromatids segregate instead of homologous chromosomes [26]. Four unique daughter cells are formed after the completion of Meiosis. The homologous recombination process takes an important role for this uniqueness.

1.1.3 Nuclear oscillation

As mentioned in the previous subsection, nuclear oscillation happens during prophase I of meiosis in fission yeast, and so as the important processes of chromosomes homologous alignment and recombination [31]. Because the impressive shape of nucleus during this stage, nuclear oscillation also often mentioned as *horse-tail* movements in biology[33, 32, 29], see in Fig. 1.4 for a time-lapse illustration. We believe the chromosome movements play an important role in this process and decide to model it quantitatively. In this subsection, we are going to elaborate the details of nuclear oscillation. We will answer the questions like what is the internal structure of nucleus during oscillation, what is the driven force of the oscillation, how long the oscillation lasts and what is the time period of the oscillation, etc.

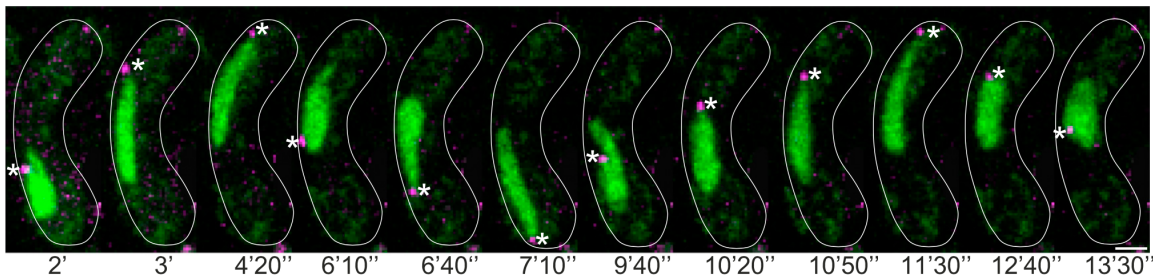


Fig. 1.4 Time-lapse experiments of nuclear oscillation in fission yeast, DNA marker in green (Rec8-GFP) and SPB marker in magenta (Sid4-mCherry) also indicated by asterisk. Reprinted from [3] with permission.

The looping structure of chromosomes: before the nuclear oscillation, chromosomes are reorganized and the bouquet formation happens. In fission yeast, the SPB is anchored in the nuclear envelope, telomeres of chromosomes are clustered to the SPB region of the inner nuclear membrane. The chromosomes are condensed to be the rod-like chain. Notice that there are still two sister chromatins contained in one chromosome. With all the telomeres bond to the SPB, chromosomes form the looping structure, as we can see in Fig. 1.3.

Redistribution of dynein motors drives the nuclear oscillation: while the inner side of SPB bonds the chromosome telomeres, the outer side is attached to the microtubules in the cytoplasm. During the oscillation, dynein motors are the energy supplier. Interestingly, as one motor is not enough for the oscillation, the collective behavior of motors is observed to drive the nucleus motion. The spatial distribution of motor molecular varies during the oscillation. Motors accumulates in the side of fission yeast that the nucleus moves toward to. It is found that the pulling force is the main contribution that drives the oscillation [13].

Related biological parameters of nuclear oscillation: to study the dynamics during oscillation, several parameters are estimated experimentally and input into our model later. These parameters are summarized in table 1.1.

Table 1.1 Parameters of fission yeast during meiosis

Parameter	Value
Typical size of nucleus	$3\mu\text{m}$
Chromosome number	Three pairs
Compaction ratio of chromatin	10^2bp/nm
Kuhn length of chromatin	$100 \sim 300\text{nm}$
Duration of nuclear oscillation	2 hours
Period of nuclear oscillation	10 min
Moving speed of nucleus	$2.5\mu\text{m/min}$
Viscosity of nucleoplasm	$1000 \times \mu_{\text{water}}$

1.1.4 The role of nuclear oscillation

Although we can clearly observe the nuclear oscillation in fission yeast, the biological role of it is not thoroughly understood. One intuitive hypothesize is that the movement facilitates the paring of homologous [16]. However, Koszul et al. proposed that the chromosome movement might play other roles than paring, such as resolve homologous entanglements or non-homologous connections [33]. Also, Mariola et al. stated a dual role for the nuclear oscillation, promoting initial paring and restricting the time of chromosome associations to ensure proper segregation [3].

We believe nuclear oscillation plays an important role for the chromosome alignment. However, it is hard to image the exact mechanism of the alignment without going deeper of the process. That is why we propose a quantitative model in this thesis and study the statistical and dynamical details of the model, trying to understand to the machinery of paring quantitatively.

1.2 Chromosomes modeled as the polymer

To quantitatively describe the chromosome, it is natural to model it as a polymer. In fact, there are already a lot of excellent examples in this direction [34–37]. However, depending on the situations under considering, different polymer models may applied.

In physics, a polymer model is usually described by beads connected by massless springs or rods. The interactions, usually characterized as different types of potentials, specify the

setting of the model [19]. As we want to model the chromosome during nuclear oscillation in fission yeast, there are two major factors we need to take into account besides some other minor details. First, the topology of the chromosome is a ring structure as shown in Fig 1.3. Second, all chromosomes are bound to the SPB and pulled by an external force. According to these biological factors and the experimental measurements like Fig. 1.3, we propose a pulled polymer loop model for the chromosomes in this specific situation. See in Fig. 1.5 for a sketch of our model. We will leave the discussion of the model details in afterward chapters.

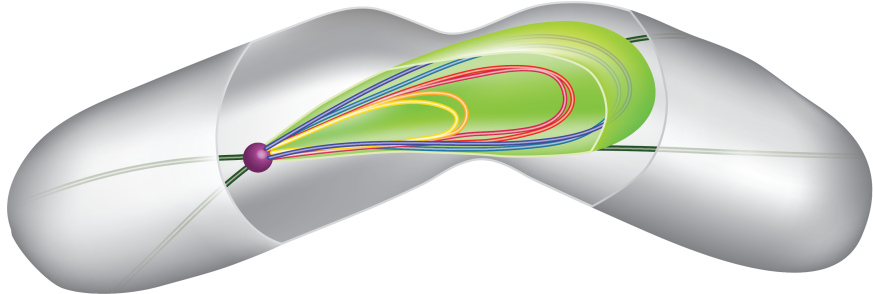


Fig. 1.5 The sketch of our pulled polymer loops model for chromosomes in meiotic fission yeast. Three pairs of chromosomes with all ends bound to SPB (shown in magenta) in the nucleus are indicated by different colors. The SPB is pulled by multiple dynein motors (not shown) walking along microtubules (dark green). The SPB is anchored to the nuclear envelope (light green) and entrains the whole nucleus.

To the best of our knowledge, there are not many works which are discussing on not only the polymer loops but also the polymer is pulled by an external force. In the following subsections, we will introduce two related aspects of previous works, i.e. works about the polymer loops and works related to pulled polymer.

1.2.1 The ring polymer model

Polymers forming a ring structure are ubiquitous in chemistry and biology [36, 38]. The study of ring polymer can go back to the years when polymer physics was built up [39, 40]. Kramers developed an equilibrium theory that possesses branch points and rings of the dilute polymer solution in 1946 [39]. Zimm calculated the statistics of mean square radii of molecules containing branches and rings in 1949 [40]. However, comparing to the simplest polymer chain model, research focus on polymer ring are far less than the former. We will review here some interesting and most related ones. Of course, it is not possible to exhaust all related works here, we pay our attention particularly to those that are related to the chromosome modeling.

Since Kramers and Zimm, there are a number of works trying to study the static and dynamical properties of the ring polymer from the theoretical point of view. In 1965, Casassa derived some statistical properties of flexible ring polymers, including mean square radius, the second Virial coefficient and angular distribution of scattering [41]. 1980, Burchard and Schmidt calculated the static and dynamical structure factors of flexible ring polymers [42]. Baumgärtner considered the self-avoiding effect of ring polymers in 1984 and found the asymptotic scaling exponents are the same as linear polymers [43]. In 1986, Cates et al. studied the nor-concatenated ring polymer melt and found the size of polymer R scales with the polymerization index N as $R \sim N^{2/5}$ and the diffusion constant D scales as $D \sim N^{-2}$ [44]. In 1994, Obukhov et al. considered the dynamics of a ring polymer in a gel and obtained the diffusion coefficient scales with the molecular weight as $D \sim M^{-2}$ and the longest relaxation time T scales as $T \sim M^{5/2}$ [45]. Carl investigated the configurational and rheological properties of multiple-twisted ring polymers using a long cyclic finitely extensible bead-spring model in 1995 [46]. He also presented a study on bead-spring chains in steady flows, various properties such like the power spectrum, the autocorrelation functions of configurational quantities were discussed in 1996 [47]. In 2001, Panyukov and Rabin studied the effects of thermal fluctuations on elastic rings. Analytical expressions are derived for some static and dynamical quantities [48]. Mukherji et al. studied a polymer ring or chain diffused around attractive surfaces. They found the diffusion constant scales as $D \sim N^{-3/2}$ linear chain and solid strong adsorbed surfaces, and $D \sim N^{-1}$ for ring polymer and soft surfaces in 2008 [49]. Sakaue proposed a simple mean-field theory for the structure of ring polymer melts which takes into account the many-body effects [50, 51]. In 2012, Kim et al. presented a self-consistent field theory formalism of topologically unconstrained ring polymers [52]. In 2013, Reigh performed lattice Monte-Carlo simulations to investigate the dependence of ring polymer conformation to the concentration, where the scaling of gyration radius with the concentration $R_g \sim \phi^{-0.59}$ was found [53]. In 2014, Lang et al. studied the tumbling dynamics of semiflexible ring polymers as a model of the cytoskeletal filament in a shear flow. They found the tumbling frequency scales f_c scales with the Weissenberg number as $f_c \sim Wi^{3/4}$ rather than the prediction of classical theory that $f_c \sim Wi^{2/3}$ [54].

Ring polymer with high concentration, like polymer melts, are often used in modeling interphase chromosomes. Interestingly, it is found that during interphase, the spatial organization for the multiple chromosomes in the nucleus is not homogeneous and well mixed. Instead, each chromosome forms its own “territories” [36]. Many interesting works can be found respecting to this problem. For example, in 2008, Rosa and Everaers used the simulation results of polymers to explain the existence and stability of territories of interphase chromosomes in genetic eukaryotes [55]. Because usually, the computation power

required to simulate the whole genome is huge, they also developed an efficient multiscale numerical approach to study the conformational statistics of ring polymers melts in [56]. Dorier employed a very simple non-permeable freely jointed polymer model and recovered the chromosomal territories in a crowded nuclei [57]. This part of work is well reviewed in [36], the interested reader can refer to the references therein.

On the other hand, it is also possible that ring polymer structures are formed temporarily in chromosomes. This could be caused by the DNA replication process or binding proteins connecting two loci of chromosomes. Many great works were done also in this direction. In 1995, Sachs use a looping random walk model to study to the interphase chromosomes, fluorescence labeled data is compared to the theoretical prediction [58]. Marko considered a model of two polymer rings tethered one another and its application to chromosome segregation in 2009 [59]. The looping probabilities of interphase chromosomes were also discussed in [60]. In 2011, Zhang et al. modeled the meiotic chromosomes as a polymer that could form internal loops by binding proteins. They found the loops play an important role in the mechanical properties of the polymer [61]. Wong set up a polymer model and use it to predict the whole nuclear architecture of fission yeast [62]. Dekker and Giorgetti employed the computational polymer model to explain the 3C/HiC data [63, 64]. In 2014, Youngren employed ring polymer model to study the duplication and segregation of *E. coli* chromosomes [65]. These are just a few examples, more can be found if one is interested.

The confinement such as the nuclear membrane or cell shape could also take an important role in chromosome dynamics. One of the examples of this kind of work is Fritzsche's work in 2011, they studied the influence of confinement geometry to the spatial organization of semiflexible ring polymers [66]. The studies of the polymers (including chains and rings) under confinements were reviewed by Ha et al. in [67].

There are also a lot of great experimental work related to ring polymers. In 1992, Tead et al. employed polystyrene molecules to perform experiments and compared the diffusion of linear and ring polymers [68]. Kapnistos et al. found the stress relaxation of entangled ring polymer was power-law rather than exponential in [69]. Structure and dynamics of polymer rings by neutron scattering were studied by Brás et al. in 2011. Witz et al. employed the atomic force microscopy to studied 2D circular DNA in [70, 71]. Gooßen et al. studied dynamics of polymer rings using neutron spin echo spectroscopy which space-time evolution of segmental motion could be observed [72, 73].

Due to its importance, the study of ring polymers is much intensive and causes much more attention nowadays. Besides what we have mentioned above, the shape of ring polymers is studied in [74–77]. Also, there are a series of works considering the ring polymer with

entanglements and topological knots [78–86]. We are only able to list a few of those great works. Interested readers can refer to the references therein.

1.2.2 Pulled polymer model

As we mentioned above, in order to model the nuclear oscillation of fission yeast, we have to consider the pulling dynamics. If we transfer the coordinate and sit on the pulled monomer, a pulled polymer is also equivalent to a pinned polymer in an external flow or force field. In this section, we would like to review some previous works in this direction. Most of them are about pulled polymer chain. Whatsoever, we think it is still helpful to know what have been done about pulled polymers or tethered polymer in an external field.

A polymer chain with one end free and the other end pulled by an external force was first discussed by de Gennes [87, 18]. After that, another important progress was made by Pincus, he developed what is now called Pincus theory [88, 89], which consider the pulled polymer as a sequence of independent “blobs”. Brochard-Wyart further developed the “trumpet” and the “stem-flower” pictures of pulled polymer chain [90, 91, 4, 92]. When the pulling force is not too strong, the polymer presents as a series of independent blobs with increasing size, i.e. the portion of polymer near to the free end fluctuates more. As the pulling force increased to a strong regime, the polymer portion near to fixed end is totally stretched, forming a “stem-flower” like picture, see in Fig. 1.6. Using fluorescence microscope and optical tweezers, Perkins et al. performed the pulling experiments on single DNA molecule and found the results consistent with the Brochard-Wyart’s theory [93, 94]. They also measured the relaxation time of this pulled polymer and obtained the scaling $\tau \sim L^{1.66}$ [95]. Wirtz also confirmed the theory by measuring transport properties of a single DNA molecule in [96].

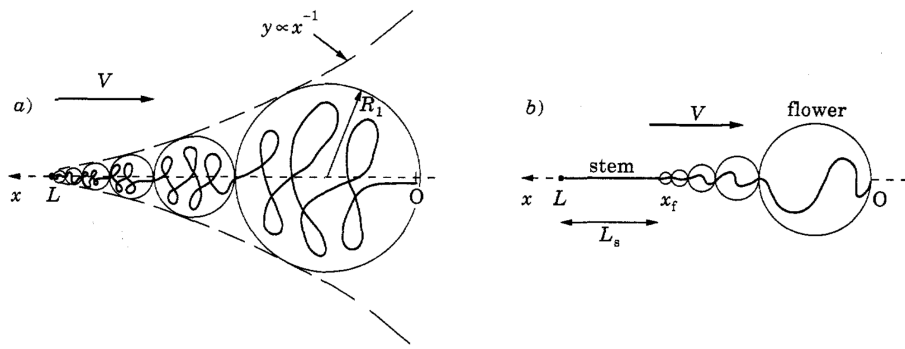


Fig. 1.6 Illustration of “stem-flower” picture for pulled polymer chain. (a) Trumpet picture at moderate pulling force; (b) Stem-flower picture at strong pulling force. Image reprinted from [4].

Rezehak et al. considered pinned polymer in a uniform flow with hydrodynamic interaction and proposed a so-called f-shell blob model [97]. Larson et al. performed Brownian Dynamics simulation for a DNA in an external flow field [98]. In 2000, Doyle measured the cyclic and stretching dynamics of a tethered DNA molecule in the shear flow [99, 100]. Sebastian studied the dynamics of pulling a polymer out of a potential well [101]. Cui performed the stretching and releasing experiment by pulling a single chicken erythrocyte chromatin fiber with the optical tweezers [102]. Rzehak discussed the conformation fluctuation and relaxation of a tethered polymer in uniform flow [103]. In 2007, Mohan et al. employed Rouse theory to study the unraveling dynamics of tethered semiflexible polymer in uniform solvent flow [104]. Sing et al. studied flexible and semiflexible tethered polymers in the limit of high shear flows and consequently near-full extension of the chains in [105]. Sakaue et al. studied the conformation and dynamics of a single flexible polymer chain that is pulled by a constant force applied at its one end, finite extensibility, the excluded volume, and the hydrodynamic interactions are discussed [106]. Varghese et al. investigated the force fluctuations in stretching a tethered polymer [107]. In 2013, Dai and Doyle found in [108] that the scenario of a pulled polymer is very similar to a polymer confined in a cylinder with proper radius.

To the best of our knowledge, the discussion of pulled ring polymer is missing except our own work [20]. So we reviewed here the works about ring polymer on one side and the works of pulled polymer on the other side. Of course, the details are not shown here, interested readers can go into the references.

1.3 Outline

With the introduction of the biological problem and the background of polymer modeling in previous two sections, we are ready to go into the details of our study. In this section, we will propose our research goals for this thesis and give an overview for the organisation of the thesis.

1.3.1 Research goals

The research goals of this thesis is listed as following:

1. Propose a polymer model to describe the chromosomes in fission yeast during nuclear oscillation. This is actually already mentioned in the previous section, i.e. the pulled polymer loop model. However, the details of the model will be discussed in the following chapters.

3. Develop the quantitative theory for our pulled looping polymer model. As far as we know, there is no previous work on this issue. On the other hand, it is shown by the experimental facts that this model is the best one for our problem.

2. Perform realistic numerical simulations of the nuclear oscillation of fission yeast using the polymer model. The theory is always simplified and has a lot of assumptions in order to analytically tractable. It is necessary to do a realistic simulation that can verify our theory on one hand, and comparable to the experimental data on the other hand.

4. Using the physical insights to understand biological processes such as chromosome alignment. Understand the biology is our ultimate goal. The chromosome movements during cell division are so important that many diseases are related to that, such as Down syndrome [109]. Our understanding from physical layer helps to fight with these diseases.

In one sentence, we want to quantitatively model the chromosome dynamics during the nuclear oscillation and use it to understand the biology.

1.3.2 Overview of the thesis

Add afterward.

Chapter 2

The Model and Simulation Methods

To model the chromosome movements during nuclear oscillation in fission yeast, let us start from a single chromosome modeled by a single polymer loop. In this chapter, we will introduce the details of the polymer model for the chromosomes and the simulation methods that resolving the dynamics and statistics of the polymer.

2.1 The pulled polymer loop model

As mentioned in the previous chapter, there are three pairs of chromosomes in fission yeast. During nuclear oscillation, these three pairs of chromosomes bound to one point, i.e. the Spindle Pole Body (SPB). Now let us start from the simplest case and neglect the interactions between chromosomes, think about a single chromosome. It is a polymer with ring structure, and an external force is exerted on the SPB. We have two choices to model this chromosome, i.e. the bead-rod model or the bead-spring model. We will use both models in this thesis but more discussions are focused on the bead-rod. Both models have their own benefits and shortcomings. Computationally, it is easier to manipulate the bead-spring model than the bead-rod. However, the bead-rod has the intrinsic property of finite extensible without resorting to some complex nonlinear spring potentials. This benefit we think is important because the chromosomes are highly condensed and are definitely finite extensible. In fact, we will show that the finite extensibility takes an important role for the polymer dynamics, see in the later chapters. And the simplicity of bead-rod model offers us the possibility to find analytical solutions.

In this section, we will introduce both the bead-rod and bead-spring model for modeling the chromosomes. However, before that, let us first do a coordinate transformation that makes our analysis much easier.

2.1.1 Coordinate transformation

Let us consider a single chromosome pulled at the SPB. The pulling force drives the chromosome moves with a velocity \mathbf{v} . In our model, the SPB is modeled as one monomer of the polymer loop. Other monomers representing the chromosome move together with the SPB because of the bonds. This scenario of pulled polymer loop is shown in Fig. 2.1 (a).

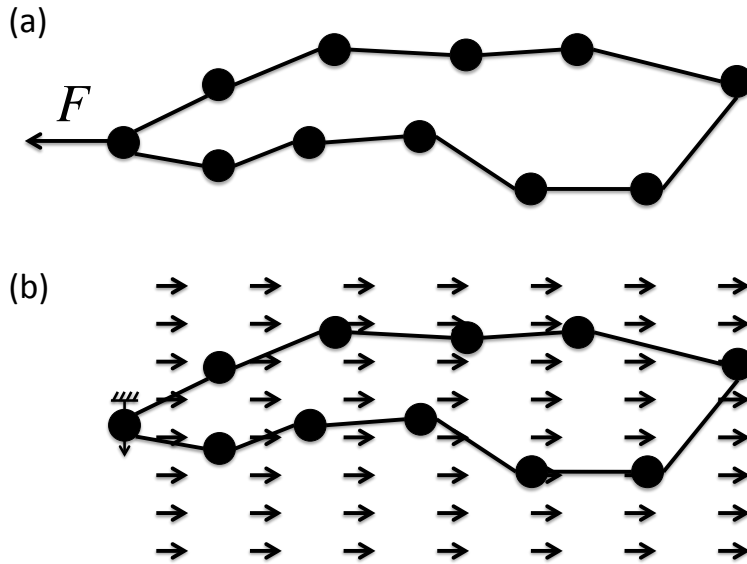


Fig. 2.1 Illustration of coordinate transformation. (a) a pulled polymer loop before transformation; (b) pinned polymer loop in an external field after transformation.

Now let us image we are sitting on the SPB. Then effectively, the SPB is pinned, and the polymer loop is immersed in a flow with velocity $-\mathbf{v}$, see in Fig. 2.1 (b). Let us assume the Stoke's law is valid and according to that, there is a force $\mathbf{F}^e = -\xi \mathbf{v}$ exerting on every bead. ξ is the friction coefficient for the bead in the solution.

In conclusion, the pulled polymer loop model is equivalent to the pinned polymer loop in an external force field. In our analysis, we will use the pinned polymer loop picture, because it is more easily to deal with both numerically and analytically.

2.1.2 The bead-rod model

Now let us come to a concrete polymer model for modeling the chromosomes, i.e. the bead-rod model. For this model, the beads representing chromosome segments are connected

by massless rigid rod. For simplicity, we assume the length of every rod is identical, denote by a . The rigidity of the rod means the distance between two neighboring beads is fixed.

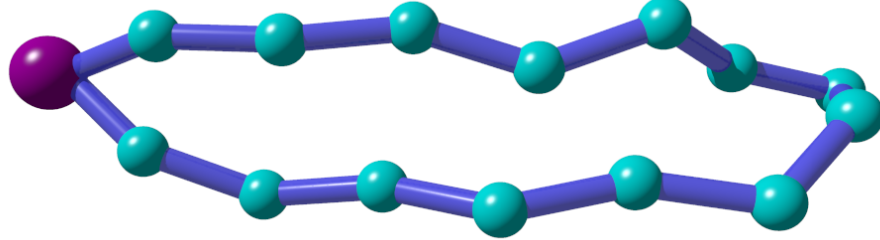


Fig. 2.2 Sketch of the bead-rod loop model. The magenta bead represents the SPB and other cyan beads represent the chromosome segments.

The dynamics of the polymer is specified by the motion of the beads. We shall first give out the dynamical equation and then explain how does it come from. Let say the contour length of the polymer loop is L , i.e. there are L beads (including the SPB) and L rods in the polymer. Denote the beads by the index $i = 0, 1, 2, \dots, L - 1$, then the dynamical equation of i^{th} bead can be written as

$$\xi \frac{d\mathbf{r}_i}{dt} = \mathbf{F}_i^u + \mathbf{F}_i^c + \mathbf{F}_i^{\text{pseudo}} + \mathbf{F}_i^e + \mathbf{F}_i^b \quad (2.1)$$

where ξ is the friction coefficient of the bead in the solution, \mathbf{F}_i^u is the interaction force specified by some kind of potentials, \mathbf{F}_i^c is the constraint force that keeps the rod length fixed, \mathbf{F}_i^e is the external force and \mathbf{F}_i^b is the Brownian force caused by thermal fluctuations. And what is left in the right hand of Eq. (2.1) is $\mathbf{F}_i^{\text{pseudo}}$, which is a special type of force introduced in the bead-rod model in order to get the correct statistics. We will discuss more about it later.

Now let us come back to explain how does Eq. (2.1) come from. Firstly, notice that \mathbf{F}_i^b in the equation is a stochastic variable, so Eq. (2.1) is actually a stochastic differential equation. Secondly, the left hand side of Eq. (2.1) is actually rearranged from the friction force of the bead in the solution $-\xi \mathbf{v}_i$. And we have assumed the solution is homogeneous so that the friction coefficient is independent of the space and time. Third, the inertial of the bead is neglected due to millions of collisions per second from the water molecules. In other word, Eq. (2.1) essentially can be written as $\mathbf{F}_i^{\text{total}} = \mathbf{0}$. This is simply the Newton's law with inertial neglected. This kind of dynamics of commonly used in polymer physics and called Brownian Dynamics [1].

Let us now discuss each term of the right hand side of Eq. (2.1) one by one.

- Brownian force \mathbf{F}_i^b

The Brownian force can be caused by the enormous instantaneous collisions of the solvent molecules or by other sort of interactions between chromosomes and proteins in the nucleus. The level of fluctuation can be characterized by an effective temperature T . Mathematically, the Brownian force is described by a Gaussian process with the zero mean in space and time and the non-zero second moment, which can be written as:

$$\langle \mathbf{F}_i^b \rangle = \mathbf{0} \quad (2.2a)$$

$$\langle \mathbf{F}_i^b(t) \mathbf{F}_j^b(t') \rangle = 2k_B T \xi \delta_{ij} \delta(t - t') \quad (2.2b)$$

here, ξ is the friction coefficient. k_B is the Boltzmann constant. δ_{ij} is the Kronecker delta means there is no correlation for the Brownian force exerting on different beads. The second δ is the Dirac delta function.

- External force \mathbf{F}_i^e

The external force in our pinned polymer loop model is simply the equivalent flow field after coordinate transformation. So we have $\mathbf{F}_i^e = \xi \mathbf{v}_{\text{SPB}}$. In general, $\mathbf{v}_{\text{SPB}} = \mathbf{v}_{\text{SPB}}(t)$ is a function of time. However, when we consider the simplest case that the chromosome is pulled to move steadily in one direction, \mathbf{v}_{SPB} is a constant.

- Constraint force \mathbf{F}_i^c

The constraint force is the tension force on the rod to keep the length fixed. So the direction of the force is along the rod orientation. The rigid rod constraint can be written as

$$|\mathbf{r}_{i+1} - \mathbf{r}_i| - a = 0 \quad (2.3)$$

where periodic index is utilized, i.e. $\mathbf{r}_L = \mathbf{r}_0$. The constraint force is an implicit force that depends on the other force exerting on the beads. We will discuss how to calculate this force in next section.

- *Pseudo* force $\mathbf{F}_i^{\text{pseudo}}$

The *Pseudo* force is special virtual force that added in order to obtain the statistics we want. If we neglect the bending energy, excluded volume effect and other complex interactions in the model, we are essentially talking about the simplest freely joint polymer model. For such a simple model, we expect the random walk statistics, i.e. the orientation of two consecutive rods is independent. So the distribution of the included angle of two rods should be uniform. However, we cannot obtain this statistics as we want without the *pseudo* force.

Let us take a simple example, the distribution of included angle of a trimer in 3D. Denote the angle as θ . The 3D spherical uniform distribution can be written as

$$p(\theta) = \text{const.} \sin \theta \quad (2.4)$$

On the other hand, the distribution of rigid bead-rod trimer without *pseudo* force can be derived using the generalized coordinate

$$p(\theta) = \text{const.} \left(1 - \frac{1}{4} \cos^2 \theta\right)^{1/2} \sin \theta \quad (2.5)$$

So they are not the same as we see here. The reason for this discrepancy is the rigidity of constraints reduce the phase space of the trimer from 6 dimensional gully to 4 dimension manifold. The simple Brownian force ensures the probability is uniform among the manifold but not θ .

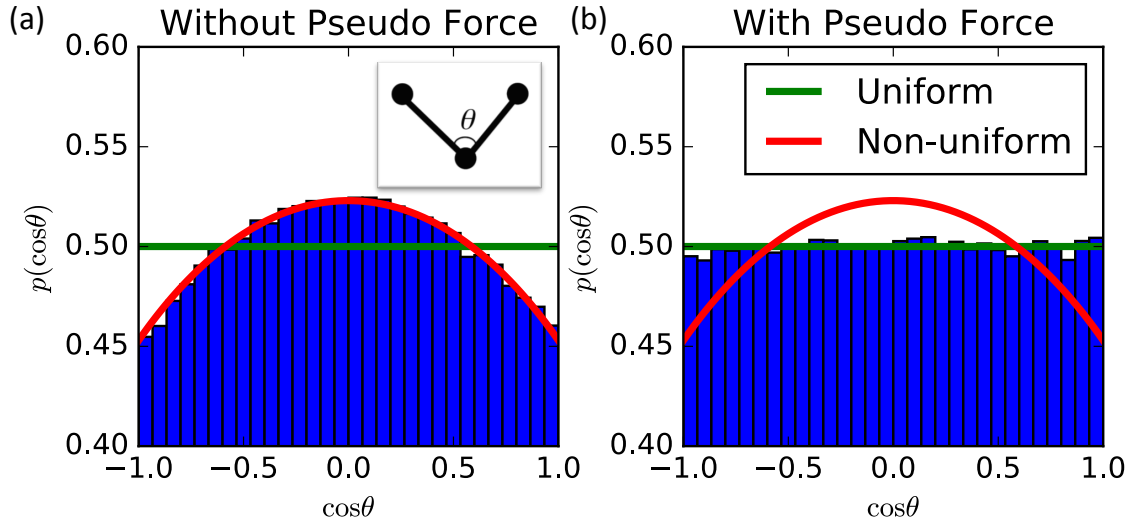


Fig. 2.3 The distribution of included angle of a bead-rod trimer. (a) without *pseudo* force; (b) with *pseudo* force. The blue bins are from Brownian Dynamics simulation results. Inset of (a) is a sketch for the trimer.

To solve the problem and obtain the statistics we want, Fixman introduced an effective *pseudo* potential depends on the polymer configuration [110], and hence we have a *pseudo* force in Eq. (2.1). The explicit form of the *pseudo* force can be written as

$$\mathbf{F}_i^{pseudo} = -\frac{\partial U_{met}}{\partial \mathbf{r}_i} \quad (2.6a)$$

$$U_{met} = \frac{1}{2}k_B T \ln(\det G) \quad (2.6b)$$

where G is the metric matrix of the bead-rod system [111]. We will show the details for the calculation of *pseudo* force in next section.

- Other potential forces \mathbf{F}_i^u

Other potential forces count the forces derived from bending energy, excluded volume effect and other interaction potentials. The general form of this force can be written as

$$\mathbf{F}_i^u = -\sum_U \frac{\partial U}{\partial \mathbf{r}_i} \quad (2.7)$$

here U can be different potentials. For instance, the bending potential can be calculated as

$$U_{bend} = -\frac{\kappa}{a} \sum_{i=1}^L \mathbf{u}_i \cdot \mathbf{u}_{i-1} \quad (2.8)$$

where $\mathbf{u}_i = |\mathbf{r}_{i+1} - \mathbf{r}_i|/a$ is the unit vector of rod orientation, κ is the bending stiffness and a is the rod length.

For excluded volume effect, we usually model this interactive as pure repulsive Lennard-Jones potential

$$U_{LJ} = \begin{cases} 4\epsilon \left[\left(\frac{\sigma}{r} \right)^{12} - \left(\frac{\sigma}{r} \right)^6 \right] & \text{if } r \leq r_c \\ 0 & \text{if } r > r_c \end{cases} \quad (2.9)$$

where r is the distance between two beads and $r_c = 2^{1/6}\sigma$, ϵ and σ are two parameters.

One can add more interaction potentials into the model. However, adding more potentials could easily lead to a complex model with many parameters. For the sake of simplicity, we will actually ignore these forces in most of our analysis. See in our later chapters.

2.1.3 The bead-spring model

The bead-spring model is another commonly used polymer model. There are several reasons that we use the bead-spring model complementary with the bead-rod model. First, the bead-spring model can work as a benchmark model of the bead-rod model. Unlike the bead-rod model, a *pseudo* force have to be added to obtain the correct random walk statistics, the model of beads connected by Hookean springs is intrinsically a system satisfied the random walk statistics. Second, we can understanding the role of finite extensibility by comparing the bead-rod and bead-spring model. Third, the computation power needed for bead-spring model is much less than the bead-rod because we avoid to calculate the *pseudo* force and implicit constraint force. Let us now look at the details of our bead-spring model.

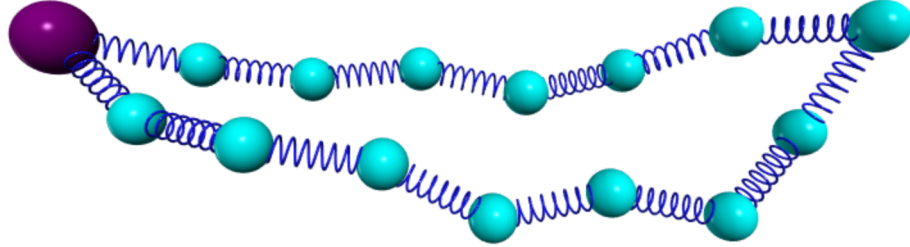


Fig. 2.4 Sketch of the bead-spring loop model. The magenta bead represents the SPB and other cyan beads represent the chromosome segments.

To model the chromosome in fission yeast during nuclear oscillation, we also need a looping structure like the bead-rod model above. The first bead represents the SPB, shown in Fig. 2.4. The dynamical equation is similar to the bead-rod model, can be written as following

$$\xi \frac{d\mathbf{r}_i}{dt} = \mathbf{F}_i^u + \mathbf{F}_i^{spring} + \mathbf{F}_i^e + \mathbf{F}_i^b \quad (2.10)$$

The notations here are the same as the bead-rod model. In addition, the Brownain force, external force and the potential force are the same as in the bead-rod model. What is different is that the *pseudo* force is not needed and the constraint force is replaced by the spring force \mathbf{F}_i^{spring} . Notice that for a bead in a loop, there are two springs connecting to it. Thus

$$\mathbf{F}_i^{spring} = F_i^s(Q_i)\mathbf{u}_i - F_{i-1}^s(Q_{i-1})\mathbf{u}_{i-1} \quad (2.11)$$

here, $F_i^s(Q_i)$ is the tension of the i^{th} spring and Q_i is the length of the spring. \mathbf{u}_i is the unit vector for the orientation of the i^{th} spring.

There are different type of springs we can use for the model. Here, we will introduce two most commonly used ones and both are used somewhere in the later chapters.

- The Hookean spring

The Hookean spring is a linear spring, where the tension of spring depends linearly on the length.

$$F^{Hookean} = H(Q - Q_0) \quad (2.12)$$

where H is the Hookean spring constant and Q_0 is the natural length of the spring. In practical Q_0 is set to a , which equals to the length of the bead-rod model. However, sometimes the zero length springs are used. We will point out when needed.

- The Finite Extensible Nonlinear Elastic (FENE) spring

The FENE spring is another commonly used spring. The force law of the spring is

$$F^{FENE} = \frac{HQ}{1 - (Q/R_0)^2} \quad (2.13)$$

here R_0 is the maximal length of the spring. As we can see in Eq. (2.13), $F^{FENE} \rightarrow \infty$ when $Q \rightarrow R_0$.

2.2 The Brownian Dynamics simulation method

After introducing the model, in this section, we will illustrate how to simulate the model numerically. Since we will plan to do most of the theoretical analysis in the later chapters and the simulation results are used to benchmark, it is convenient that we show the methods of simulation before that.

The Brownian Dynamics (BD) simulation is a kind of Molecule Dynamics (MD) simulation technique. The governing equation of each monomer or particle is integrated to get the trajectories. And physical quantities are measured by ensemble average over trajectories of thousands of monomers. In our situation, the governing equations are Eq. (2.1) or Eq. (2.10). Our interested quantities are something like the average space distance between two beads, the typical size of the polymer and the characteristic time scale of the system dynamics. These are all tractable by BD simulations.

In the following subsections, we will introduce the algorithms used to do the bead-rod and bead-spring simulation separately. The simulation code is implemented in C++2011. Most the simulation are computed in our clusters with X86 architecture.

2.2.1 BD simulation of the bead-rod model

The goal of simulation is essentially to solve the first order ordinary stochastic differential equation Eq. (2.1) numerically. However, the simple integration algorithm such as the Euler algorithm would not work here. This is because of the implicit constraint force \mathbf{F}_i^c . Here we employ the predictor-corrector algorithm introduced by Liu [112].

To simplify the illustration of the algorithm, we will ignore all complex potential forces and the external force in Eq. (2.1), i.e. $\mathbf{F}_i^u = \mathbf{F}_i^e = \mathbf{0}$. It is easy to add them back after knowing the algorithm. The dynamical equation after simplification looks

$$\frac{d\mathbf{r}_i}{dt} = \frac{1}{\xi} \left(\mathbf{F}_i^c + \mathbf{F}_i^{pseudo} + \mathbf{F}_i^b \right) \quad (2.14)$$

The predictor-corrector algorithm is a two step algorithm and can be divided into the predict step and correct step. In the predict step, the next time step position is evaluated without considering the constraints

$$\mathbf{r}_i^*(t + \Delta t) = \mathbf{r}_i(t) + \frac{1}{\xi} (\mathbf{F}_i^{pseudo} + \mathbf{F}_i^b) \Delta t \quad (2.15)$$

In order to do the calculation, we need to evaluate the Brownian force and the *pseudo* force first. Here we will show how to do that one by one.

- Evaluation of the Brownain force \mathbf{F}_i^b
- Evaluation of the *pseudo* force \mathbf{F}_i^{pseudo}

2.2.2 BD simulation of the bead-spring model

And we nondimensionalize the dynamical equation by rescaling the variable in the following way:

$$\mathbf{r}' \rightarrow \mathbf{r}/a; t' \rightarrow t/(\xi a^2/k_B T); \mathbf{F}' \rightarrow \mathbf{F}/(k_B T/a). \quad (2.16)$$

After the rescaling, the length unit is set to the size of the rod. Without causing of confusing, we will ignore the prime in our notation.

2.3 The Monte-Carlo simulation of the bead-rod model

2.4 Summary

Chapter 3

Simulation Methods

3.1 Brownian Dynamics Simulation of the Bead-rod Model

3.1.1 Predictor-corrector Algorithm

3.1.2 The Pseudo Force

3.2 Monte-Carlo Simulation of the Bead-rod Model

3.3 Brownian Dynamics Simulation of the Bead-spring Model

3.3.1 Euler Algorithm and Stochastic Runge-Kutta Algorithm

3.3.2 Excluded volume

3.3.3 Bending Potential

3.4 Monte-Carlo Simulation of the Particle Hopping Model

3.4.1 Classical Monte-Carlo

3.4.2 Kinetic Monte-Carlo

3.5 Summary

Chapter 4

Equilibrium Statistics

4.1 Pinned Polymer Loop Model

4.1.1 Polymer Loop Moving in One Direction

4.1.2 Pinned Polymer Loop in Constant Force Field

4.2 Pinned Polymer Loop in 1D

4.2.1 Mapping to Particles on 1D Lattice

4.2.2 The Grand Canonical Ensemble Solution

The Fermi-Dirac Statistics

The Brownian Bridge Condition

4.2.3 Canonical Ensemble Solution

The Number Partition Theory

Exact Partition Function

4.3 Equilibrium Statistics in 3D

4.3.1 The Mean of Bead Position

4.3.2 The Variance of Bead Position

4.4 Two intersecting Loops

4.5 Back to the Biological Problem

4.6 Summary

Chapter 5

Dynamical Properties

5.1 Rouse Theory of the Pinned Bead-spring Loop

5.1.1 The Normal Modes

5.1.2 Relaxation Time

5.2 1D Pinned Bead-rod Loop Maps to ASEP

5.3 The Bethe-ansatz Solution of ASEP

5.3.1 Solution of Single Particle

5.3.2 Solution of Two Particles

5.3.3 Solution of General N particles

5.3.4 Relaxation Time

5.4 Relaxation Time of 3D Pinned Bead-rod Loop

5.5 The Single-file Diffusion

5.6 Summary

Chapter 6

Characterize the Nuclear Oscillation

6.1 Oscillation of the Pinned Polymer Loop

6.1.1 The Rouse Theory

6.1.2 Simulation Results

6.2 Characterize the Shape of Chromosomes

6.2.1 The Gyration Tensor

6.2.2 Asphericity and the Nature of Asphericity

6.3 Extract Shape Information From Experimental Data

6.3.1 Shape from Experimental Data

6.3.2 Compare to Theory and Simulation Results

6.4 Summary

Chapter 7

Conclusions and Outlook

7.1 Conclusions

7.2 Outlook

Appendix A

The Toeplitz Matrix

Appendix B

The Bethe-ansatz Solution of Periodic ASEP

References

- [1] D O Morgan. *The Cell Cycle: Principles of Control*. Primers in Biology. OUP/New Science Press, 2007.
- [2] Haruhiko Asakawa, Tokuko Haraguchi, and Yasushi Hiraoka. Reconstruction of the kinetochore: a prelude to meiosis. *Cell Div.*, 2(1):17, 2007.
- [3] Mariola R. Chacón, Petrina Delivani, and Iva M. Tolić. Meiotic Nuclear Oscillations Are Necessary to Avoid Excessive Chromosome Associations. *Cell Rep.*, 17(6):1632–1645, nov 2016.
- [4] F. Brochard-Wyart. Polymer Chains Under Strong Flows: Stems and Flowers. *Europhys. Lett.*, 30(7):387–392, jun 1995.
- [5] Carolyn T. MacDonald, Julian H. Gibbs, and Allen C. Pipkin. Kinetics of Biopolymerization. *Biopolymers*, 6:1–25, 1968.
- [6] Paul C. Bressloff, Jay M. Newby, and B. Derrida. Stochastic models of intracellular transport. *Rev. Mod. Phys.*, 301(1-3):135–196, 2013.
- [7] T Chou, K Mallick, and R K P Zia. Non-equilibrium statistical mechanics: from a paradigmatic model to biological transport. *Reports Prog. Phys.*, 74(11):116601, nov 2011.
- [8] Alan A Berryman. The Origins and Evolution of Predator-Prey Theory. *Ecology*, 73(5):1530–1535, oct 1992.
- [9] Thomas Butler and Nigel Goldenfeld. Robust ecological pattern formation induced by demographic noise. *Phys. Rev. E*, 80(3):030902, sep 2009.
- [10] G. Sugihara, R. May, H. Ye, C.-h. Hsieh, E. Deyle, M. Fogarty, and S. Munch. Detecting Causality in Complex Ecosystems. *Science (80-.).*, 338(6106):496–500, oct 2012.
- [11] Jennifer L Williams, Bruce E Kendall, and Jonathan M Levine. Rapid evolution accelerates plant population spread in fragmented experimental landscapes. *Science (80-.).*, 353(6298):482–485, jul 2016.
- [12] Y Chikashige, D. Ding, H Funabiki, T Haraguchi, S Mashiko, M Yanagida, and Y Hiraoka. Telomere-led premeiotic chromosome movement in fission yeast. *Science (80-.).*, 264(5156):270–273, apr 1994.

- [13] Sven K Vogel, Nenad Pavin, Nicola Maghelli, Frank Jülicher, and Iva M Tolić-Nørrelykke. Self-Organization of Dynein Motors Generates Meiotic Nuclear Oscillations. *PLoS Biol.*, 7(4):e1000087, apr 2009.
- [14] Hiroki Shibuya, Akihiro Morimoto, and Yoshinori Watanabe. The Dissection of Meiotic Chromosome Movement in Mice Using an In Vivo Electroporation Technique. *PLoS Genet.*, 10(12):e1004821, 2014.
- [15] A Yamamoto, C Tsutsumi, H Kojima, K Oiwa, and Y Hiraoka. Dynamic Behavior of Microtubules during Dynein-dependent Nuclear Migrations of Meiotic Prophase in Fission Yeast. *Mol. Biol. Cell*, 12(12):3933–3946, dec 2001.
- [16] Da-Qiao Ding, Ayumu Yamamoto, Tokuko Haraguchi, and Yasushi Hiraoka. Dynamics of Homologous Chromosome Pairing during Meiotic Prophase in Fission Yeast. *Dev. Cell*, 6(3):329–341, mar 2004.
- [17] Jennifer L Gerton and R Scott Hawley. Homologous chromosome interactions in meiosis: diversity amidst conservation. *Nat. Rev. Genet.*, 6(6):477–487, jun 2005.
- [18] Pierre-Gilles G de Gennes. *Scaling Concepts in Polymer Physics*. Cornell University Press, 1979.
- [19] M. Doi and S. F. Edwards. *The theory of polymer dynamics*. Oxford University Press, 1988.
- [20] Yen Ting Lin, Daniela Frömberg, Wenwen Huang, Petrina Delivani, Mariola Chacón, Iva M. Tolić, Frank Jülicher, and Vasily Zaburdaev. Pulled Polymer Loops as a Model for the Alignment of Meiotic Chromosomes. *Phys. Rev. Lett.*, 115(20):208102, nov 2015.
- [21] Susan L Forsburg. Overview of *Schizosaccharomyces pombe*. In *Curr. Protoc. Mol. Biol.*, volume Chapter 13, page Unit 13.14. 2003.
- [22] Peter A. Fantes and Charles S. Hoffman. A Brief History of *Schizosaccharomyces pombe* Research: A Perspective Over the Past 70 Years. *Genetics*, 203(2):621–629, jun 2016.
- [23] Charles S. Hoffman, Valerie Wood, and Peter A. Fantes. An Ancient Yeast for Young Geneticists: A Primer on the *Schizosaccharomyces pombe* Model System. *Genetics*, 201(2):403–423, oct 2015.
- [24] V. Wood, R. Gwilliam, M.-A. Rajandream, M. Lyne, R. Lyne, A. Stewart, J. Sgouros, N. Peat, J. Hayles, S. Baker, D. Basham, S. Bowman, K. Brooks, D. Brown, S. Brown, T. Chillingworth, C. Churcher, M. Collins, R. Connor, A. Cronin, P. Davis, T. Feltwell, A. Fraser, S. Gentles, A. Goble, N. Hamlin, D. Harris, J. Hidalgo, G. Hodgson, S. Holroyd, T. Hornsby, S. Howarth, E. J. Huckle, S. Hunt, K. Jagels, K. James, L. Jones, M. Jones, S. Leather, S. McDonald, J. McLean, P. Mooney, S. Moule, K. Mungall, L. Murphy, D. Niblett, C. Odell, K. Oliver, S. O’Neil, D. Pearson, M. A. Quail, E. Rabinowitzsch, K. Rutherford, S. Rutter, D. Saunders, K. Seeger, S. Sharp, J. Skelton, M. Simmonds, R. Squares, S. Squares, K. Stevens, K. Taylor,

- R. G. Taylor, A. Tivey, S. Walsh, T. Warren, S. Whitehead, J. Woodward, G. Volckaert, R. Aert, J. Robben, B. Grymonprez, I. Weltjens, E. Vanstreels, M. Rieger, M. Schäfer, S. Müller-Auer, C. Gabel, M. Fuchs, C. Fritz, E. Holzer, D. Moestl, H. Hilbert, K. Borzym, I. Langer, A. Beck, H. Lehrach, R. Reinhardt, T. M. Pohl, P. Eger, W. Zimmermann, H. Wedler, R. Wambutt, B. Purnelle, A. Goffeau, E. Cadieu, S. Dréano, S. Gloux, V. Lelaure, S. Mottier, F. Galibert, S. J. Aves, Z. Xiang, C. Hunt, K. Moore, S. M. Hurst, M. Lucas, M. Rochet, C. Gaillardin, V. A. Tallada, A. Garzon, G. Thode, R. R. Daga, L. Cruzado, J. Jimenez, M. Sánchez, F. del Rey, J. Benito, A. Domínguez, J. L. Revuelta, S. Moreno, J. Armstrong, S. L. Forsburg, L. Cerrutti, T. Lowe, W. R. McCombie, I. Paulsen, J. Potashkin, G. V. Shpakovski, D. Ussery, B. G. Barrell, and P. Nurse. The genome sequence of *Schizosaccharomyces pombe*. *Nature*, 415(6874):871–880, feb 2002.
- [25] Miguel Coelho, Aygül Dereli, Anett Haese, Sebastian Kühn, Liliana Malinovska, Morgan E. DeSantis, James Shorter, Simon Alberti, Thilo Gross, and Iva M. Tolić-Nørrelykke. Fission Yeast Does Not Age under Favorable Conditions, but Does So after Stress. *Curr. Biol.*, 23(19):1844–1852, oct 2013.
- [26] S Freeman. *Biological Science*. Pearson/Benjamin Cummings, 2008.
- [27] a M Villeneuve and K J Hillers. Whence meiosis? *Cell*, 106(6):647–650, 2001.
- [28] David M. Richards, Emma Greer, Azahara C. Martin, Graham Moore, Peter J. Shaw, and Martin Howard. Quantitative Dynamics of Telomere Bouquet Formation. *PLoS Comput. Biol.*, 8(12):e1002812, dec 2012.
- [29] L Davis and G R Smith. Meiotic recombination and chromosome segregation in *Schizosaccharomyces pombe*. *Proc. Natl. Acad. Sci.*, 98(15):8395–8402, jul 2001.
- [30] Osami Niwa, Mizuki Shimanuki, and Futaba Miki. Telomere-led bouquet formation facilitates homologous chromosome pairing and restricts ectopic interaction in fission yeast meiosis. *EMBO J.*, 19(14):3831–3840, jul 2000.
- [31] D Q Ding, Y Chikashige, T Haraguchi, and Y Hiraoka. Oscillatory nuclear movement in fission yeast meiotic prophase is driven by astral microtubules, as revealed by continuous observation of chromosomes and microtubules in living cells. *J. Cell Sci.*, 111 (Pt 6):701–12, mar 1998.
- [32] Jennifer L. Wells, David W. Pryce, and Ramsay J. McFarlane. Homologous chromosome pairing in *Schizosaccharomyces pombe*. *Yeast*, 23(13):977–989, oct 2006.
- [33] Romain Koszul and Nancy Kleckner. Dynamic chromosome movements during meiosis: a way to eliminate unwanted connections? *Trends Cell Biol.*, 19(12):716–724, 2009.
- [34] Hua Wong, Jean-michel Arbona, and Christophe Zimmer. How to build a yeast nucleus. *Nucleus*, 4(5):361–366, sep 2013.
- [35] Douglas R. Tree, Abhiram Muralidhar, Patrick S. Doyle, and Kevin D. Dorfman. Is DNA a Good Model Polymer. *Macromolecules*, 46(20):8369–8382, oct 2013.

- [36] Jonathan D Halverson, Jan Smrek, Kurt Kremer, and Alexander Y Grosberg. From a melt of rings to chromosome territories: the role of topological constraints in genome folding. *Reports Prog. Phys.*, 77(2):022601, feb 2014.
- [37] Suckjoon Jun and Andrew Wright. Entropy as the driver of chromosome segregation. *Nat. Rev. Microbiol.*, 8(8):600–607, 2010.
- [38] D. Richter, S. Gooßen, and A. Wischnewski. Celebrating Soft Matter’s 10th Anniversary: Topology matters: structure and dynamics of ring polymers. *Soft Matter*, 11(44):8535–8549, 2015.
- [39] H. A. Kramers. The Behavior of Macromolecules in Inhomogeneous Flow. *J. Chem. Phys.*, 14(7):415–424, jul 1946.
- [40] Bruno H. Zimm and Walter H. Stockmayer. The Dimensions of Chain Molecules Containing Branches and Rings. *J. Chem. Phys.*, 17(12):1301–1314, 1949.
- [41] Edward F. Casassa. Some statistical properties of flexible ring polymers. *J. Polym. Sci. Part A Gen. Pap.*, 3(2):605–614, feb 1965.
- [42] W BURCHARD and M SCHMIDT. Static and dynamic structure factors calculated for flexible ring macromolecules. *Polymer (Guildf.)*, 21(7):745–749, jul 1980.
- [43] A. Baumg\{"o\}rtner. Statistics of self-avoiding ring polymers. *J. Chem. Phys.*, 76(8):4275, nov 1982.
- [44] M.E. Cates and J.M. Deutsch. Conjectures on the statistics of ring polymers. *J. Phys.*, 47(12):2121–2128, 1986.
- [45] Sergei P. Obukhov, Michael Rubinstein, and Thomas Duke. Dynamics of a Ring Polymer in a Gel. *Phys. Rev. Lett.*, 73(9):1263–1266, aug 1994.
- [46] Wilfried Carl. Configurational and rheological properties of cyclic polymers. *J. Chem. Soc. Faraday Trans.*, 91(16):2525–2530, 1995.
- [47] W. Carl. Some aspects of theory and simulations of polymers in steady flows. *Macromol. Theory Simulations*, 5(1):1–27, 1996.
- [48] Sergey Panyukov and Yitzhak Rabin. Fluctuating elastic rings: Statics and dynamics. *Phys. Rev. E*, 64(1):011909, jun 2001.
- [49] Debashish Mukherji, Guido Bartels, and Martin H. Müser. Scaling laws of single polymer dynamics near attractive surfaces. *Phys. Rev. Lett.*, 100(February):1–4, 2008.
- [50] Takahiro Sakaue. Ring polymers in melts and solutions: Scaling and crossover. *Phys. Rev. Lett.*, 106(April):1–4, 2011.
- [51] Takahiro Sakaue. Statistics and geometrical picture of ring polymer melts and solutions. *Phys. Rev. E*, 85(2):021806, feb 2012.
- [52] Jaeup U. Kim, Yong-Biao Yang, and Won Bo Lee. Self-Consistent Field Theory of Gaussian Ring Polymers. *Macromolecules*, 45(7):3263–3269, apr 2012.

- [53] Shang Yik Reigh and Do Y. Yoon. Concentration Dependence of Ring Polymer Conformations from Monte Carlo Simulations. *ACS Macro Lett.*, 2(4):296–300, apr 2013.
- [54] Philipp S. Lang, Benedikt Obermayer, and Erwin Frey. Dynamics of a semiflexible polymer or polymer ring in shear flow. *Phys. Rev. E*, 89(2):022606, feb 2014.
- [55] Angelo Rosa and Ralf Everaers. Structure and Dynamics of Interphase Chromosomes. *PLoS Comput. Biol.*, 4(8):e1000153, aug 2008.
- [56] Angelo Rosa and Ralf Everaers. Ring Polymers in the Melt State: The Physics of Crumpling. *Phys. Rev. Lett.*, 112(11):118302, mar 2014.
- [57] Julien Dorier and Andrzej Stasiak. Topological origins of chromosomal territories. *Nucleic Acids Res.*, 37(19):6316–6322, oct 2009.
- [58] R K Sachs, G van den Engh, B Trask, H Yokota, and J E Hearst. A random-walk/giant-loop model for interphase chromosomes. *Proc. Natl. Acad. Sci.*, 92(7):2710–2714, mar 1995.
- [59] John F Marko. Linking topology of tethered polymer rings with applications to chromosome segregation and estimation of the knotting length. *Phys. Rev. E*, 79(5):051905, may 2009.
- [60] Angelo Rosa, Nils B Becker, and Ralf Everaers. Looping probabilities in model interphase chromosomes. *Biophys. J.*, 98(11):2410–9, jun 2010.
- [61] Yang Zhang and Dieter W. Heermann. Loops determine the mechanical properties of mitotic chromosomes. *PLoS One*, 6(12):e29225, dec 2011.
- [62] Hua Wong, Hervé Marie-Nelly, Sébastien Herbert, Pascal Carrivain, Hervé Blanc, Romain Koszul, Emmanuelle Fabre, and Christophe Zimmer. A Predictive Computational Model of the Dynamic 3D Interphase Yeast Nucleus. *Curr. Biol.*, 22(20):1881–1890, oct 2012.
- [63] Job Dekker, Marc a Marti-Renom, and Leonid a Mirny. Exploring the three-dimensional organization of genomes: interpreting chromatin interaction data. *Nat. Rev. Genet.*, 14(6):390–403, may 2013.
- [64] Luca Giorgietti, Rafael Galupa, Elphège P Nora, Tristan Piolot, France Lam, Job Dekker, Guido Tiana, and Edith Heard. Predictive polymer modeling reveals coupled fluctuations in chromosome conformation and transcription. *Cell*, 157(4):950–63, may 2014.
- [65] Brenda Youngren, Henrik Jörk Nielsen, Suckjoon Jun, and Stuart Austin. The multi-fork Escherichia coli chromosome is a self-duplicating and self-segregating thermodynamic ring polymer. *Genes Dev.*, 28:71–84, 2014.
- [66] Miriam Fritzsche and Dieter W. Heermann. Confinement driven spatial organization of semiflexible ring polymers: Implications for biopolymer packaging. *Soft Matter*, 7(15):6906, 2011.

- [67] Bae-Yeon Ha and Youngkyun Jung. Polymers under confinement: single polymers, how they interact, and as model chromosomes. *Soft Matter*, 11(12):2333–2352, 2015.
- [68] S. F. Tead, E. J. Kramer, G. Hadzioannou, M. Antonietti, H. Sillescu, P. Lutz, and C. Strazielle. Polymer topology and diffusion: a comparison of diffusion in linear and cyclic macromolecules. *Macromolecules*, 25(15):3942–3947, jul 1992.
- [69] M Kapnistos, M Lang, D Vlassopoulos, W Pyckhout-Hintzen, D Richter, D Cho, T Chang, and M Rubinstein. Unexpected power-law stress relaxation of entangled ring polymers. *Nat. Mater.*, 7(12):997–1002, dec 2008.
- [70] Guillaume Witz, Kristian Rechendorff, Jozef Adamcik, and Giovanni Dietler. Conformation of circular DNA in two dimensions. *Phys. Rev. Lett.*, 101(14):3–6, 2008.
- [71] G. Witz, K. Rechendorff, J. Adamcik, and G. Dietler. Conformation of ring polymers in 2D constrained environments. *Phys. Rev. Lett.*, 106(June):2–5, 2011.
- [72] S Gooßen, ARE Brás, M Krutyeva, M Sharp, P Falus, A Feoktystov, U Gasser, W. Pyckhout-Hintzen, A Wischnewski, and D Richter. Molecular Scale Dynamics of Large Ring Polymers. *Phys. Rev. Lett.*, 113(16):168302, oct 2014.
- [73] Sebastian Gooßen, Margarita Krutyeva, Melissa Sharp, Artem Feoktystov, Jürgen Allgaier, Wim Pyckhout-Hintzen, Andreas Wischnewski, and Dieter Richter. Sensing Polymer Chain Dynamics through Ring Topology: A Neutron Spin Echo Study. *Phys. Rev. Lett.*, 115(14):148302, 2015.
- [74] Marvin Bishop and J. P. J. Michels. The shape of ring polymers. *J. Chem. Phys.*, 82(2):1059–1061, jan 1985.
- [75] O. Jagodzinski, E. Eisenriegler, and K. Kremer. Universal shape properties of open and closed polymer chains: renormalization group analysis and Monte Carlo experiments. *J. Phys. I Fr.*, 2:2243–2279, 1992.
- [76] Karen Alim and Erwin Frey. Shapes of semiflexible polymer rings. *Phys. Rev. Lett.*, 99(November):1–4, 2007.
- [77] Pascal Reiss, Miriam Fritzsche, and Dieter W. Heermann. Looped star polymers show conformational transition from spherical to flat toroidal shapes. *Phys. Rev. E*, 84(5):051910, nov 2011.
- [78] J.P.J. Michels and F.W. Wiegel. Probability of knots in a polymer ring. *Phys. Lett. A*, 90(7):381–384, 1982.
- [79] Kleanthes Koniaris and M. Muthukumar. Knottedness in ring polymers. *Phys. Rev. Lett.*, 66(17):2211–2214, 1991.
- [80] Kleanthes Koniaris and M. Muthukumar. Self-entanglement in ring polymers. *J. Chem. Phys.*, 95(4):2873, 1991.
- [81] Alexander Grosberg, Alexander Feigel, and Yitzhak Rabin. Flory-type theory of a knotted ring polymer. *Phys. Rev. E*, 54(6):6618–6622, 1996.

- [82] Miyuki K Shimamura and Tetsuo Deguchi. Gyration radius of a circular polymer under a topological constraint with excluded volume. *Phys. Rev. E*, 64(2):020801, jul 2001.
- [83] E Orlandini, a L Stella, and C Vanderzande. Polymer θ -point as a knot delocalization transition. *Phys. Rev. E*, 68(3):031804, sep 2003.
- [84] Luca Tubiana, Enzo Orlandini, and Cristian Micheletti. Multiscale entanglement in ring polymers under spherical confinement. *Phys. Rev. Lett.*, 107(October):1–4, 2011.
- [85] Erica Uehara and Tetsuo Deguchi. Statistical and hydrodynamic properties of double-ring polymers with a fixed linking number between twin rings. *J. Chem. Phys.*, 140(4), 2014.
- [86] Bing Li, Zhao-Yan Yan Sun, and Li-Jia Jia An. Effects of topology on the adsorption of singly tethered ring polymers to attractive surfaces. *J. Chem. Phys.*, 143(2):024908, 2015.
- [87] P. G. De Gennes. Coil-stretch transition of dilute flexible polymers under ultrahigh velocity gradients. *J. Chem. Phys.*, 60(12):5030–5042, jun 1974.
- [88] P Pincus. Excluded Volume Effects and Stretched Polymer Chains. *Macromolecules*, 9(3):386–388, may 1976.
- [89] P. Pincus. Dynamics of Stretched Polymer Chains. *Macromolecules*, 10(1):210–213, jan 1977.
- [90] F Brochard-Wyart. Deformations of One Tethered Chain in Strong Flows. *Europhys. Lett.*, 23(2):105–111, jul 1993.
- [91] F Brochard-Wyart, H Hervet, and P Pincus. Unwinding of Polymer Chains under Forces or Flows. *Europhys. Lett.*, 26(7):511–516, jun 1994.
- [92] A Adjarei, F Brochardt-Wyart, and P G de Gennes. Drag on a Tethered Chain in a Polymer Melt. *J. Phys. II Fr.*, 5:491, 1995.
- [93] Thomas Perkins, Douglas Smith, Ronald Larson, and Steven Chu. Stretching of a single tethered polymer in a uniform flow. *Science (80-.).*, 268(5207):83–87, apr 1995.
- [94] T. Perkins, D. Smith, and S Chu. Direct observation of tube-like motion of a single polymer chain. *Science (80-.).*, 264(5160):819–822, may 1994.
- [95] T. Perkins, Quake, D. Smith, and S Chu. Relaxation of a single DNA molecule observed by optical microscopy. *Science (80-.).*, 264(5160):822–826, may 1994.
- [96] D Wirtz. Direct Measurement of the Transport-Properties of a Single DNA Molecule. *Phys. Rev. Lett.*, 75(12):2436–2439, 1995.
- [97] R Rzehak, D Kienle, T Kawakatsu, and W Zimmermann. Partial draining of a tethered polymer in flow. *Europhys. Lett.*, 46(6):821–826, jun 1999.

- [98] R. G. Larson, Hua Hu, D. E. Smith, and S. Chu. Brownian dynamics simulations of a DNA molecule in an extensional flow field. *J. Rheol. (N. Y. N. Y.)*, 43(2):267, 1999.
- [99] P S Doyle, B Ladoux, and J L Viovy. Dynamics of a tethered polymer in shear flow. *Phys. Rev. Lett.*, 84(20):4769–4772, 2000.
- [100] B Ladoux and P S Doyle. Stretching tethered DNA chains in shear flow. *Europhys. Lett.*, 52(5):511–517, dec 2000.
- [101] K L Sebastian. Pulling a polymer out of a potential well and the mechanical unzipping of DNA. *Phys. Rev. E*, 62(1):1128–1132, jul 2000.
- [102] Y Cui and C Bustamante. Pulling a single chromatin fiber reveals the forces that maintain its higher-order structure. *Proc. Natl. Acad. Sci.*, 97(1):127–132, jan 2000.
- [103] R Rzehak. Conformational fluctuations of a tethered polymer in uniform flow. *Eur. Phys. J. E - Soft Matter*, 11(4):335–348, aug 2003.
- [104] Aruna Mohan and Patrick S Doyle. Unraveling of a Tethered Polymer Chain in Uniform Solvent Flow. *Macromolecules*, 40(12):4301–4312, jun 2007.
- [105] Charles E. Sing and Alfredo Alexander-Katz. Theory of tethered polymers in shear flow: The strong stretching limit. *Macromolecules*, 44(22):9020–9028, 2011.
- [106] Takahiro Sakaue, Takuya Saito, and Hirofumi Wada. Dragging a polymer in a viscous fluid: Steady state and transient. *Phys. Rev. E*, 86(1):011804, jul 2012.
- [107] Anoop Varghese, Satyavani Vemparala, and R. Rajesh. Force fluctuations in stretching a tethered polymer. *Phys. Rev. E*, 88(2):022134, 2013.
- [108] Liang Dai and Patrick S. Doyle. Comparisons of a polymer in confinement versus applied force. *Macromolecules*, 46(15):6336–6344, 2013.
- [109] David Patterson. Molecular genetic analysis of Down syndrome. *Hum. Genet.*, 126(1):195–214, jul 2009.
- [110] M. Fixman. Classical Statistical Mechanics of Constraints: A Theorem and Application to Polymers. *Proc. Natl. Acad. Sci.*, 71(8):3050–3053, 1974.
- [111] Matteo Pasquali and David C. Morse. An efficient algorithm for metric correction forces in simulations of linear polymers with constrained bond lengths. *J. Chem. Phys.*, 116(5):1834, 2002.
- [112] Tony W. Liu. Flexible polymer chain dynamics and rheological properties in steady flows. *J. Chem. Phys.*, 90(10):5826, 1989.